Original paper

Effect of a lead block on alveolar bone protection in image-guided high-dose-rate interstitial brachytherapy for tongue cancer: using model-based dose calculation algorithms to correct for inhomogeneity

Hironori Akiyama, DDS[1], Ken Yoshida, MD[2], Tadashi Takenaka, RTT[3], Tadayuki Kotsuma, MD[4], Koji Masui, MD[5], Hajime Monzen, PhD[6], Iori Sumida, PhD[7], Yutaka Tsujimoto, RTT[8], Mamoru Miyao, RTT[9], Hiroki Okumura, RTT[9], Taiju Shimbo, MD[9], Hideki Takegawa, Msc[10], Naoya Murakami, MD[11], Koji Inaba, MD[11], Tairo Kashihara, MD[11], Zoltán Takácsi-Nagy, MD[12], Nikolaos Tselis, MD[13], Hideya Yamazaki, MD[3], Eiichi Tanaka, MD[8], Keiji Nihei, MD[9], Yoshiko Ariji, DDS[1]

[1]Department of Oral Radiology, Osaka Dental University, Osaka, Japan, [2]Department of Radiology, Kansai Medical University Medical Center, Osaka, Japan, [3]Department of Radiology, Graduate School of Medical Science, Kyoto Prefectural University of Medicine, Kyoto, Japan, [4]Department of Radiation Oncology, Osaka Rosai Hospital, Osaka, Japan, [5]Department of Radiology, Fukuchiyama City Hospital, Kyoto, Japan, [6]Department of Medical Physics, Graduate School of Medical Sciences, Kindai University, Osaka, Japan, [7]Department of Radiation Oncology, Graduate School of Medicine, Osaka University, Osaka, Japan, [8]Department of Radiation Oncology, National Hospital Organization Osaka National Hospital, Osaka, Japan, [9]Department of Radiation Oncology, Osaka Medical and Pharmaceutical University, Osaka, Japan, [10]Department of Radiology, Kansai Medical University, Osaka, Japan, [11]Department of Radiation Oncology, National Cancer Center Hospital, Tokyo, Japan, [12]Center of Radiotherapy, National Institute of Oncology, Department of Oncology, Semmelweis University, Budapest, Hungary, [13]Department of Radiotherapy and Oncology, University Hospital Frankfurt, Goethe University Frankfurt, Frankfurt am Main, Germany

The research was conducted at 2-7 Daigaku-machi, Takatsuki, Osaka, 569-8686, Japan.

Abstract

Purpose: The purpose of this study was to evaluate the effect of a lead block for alveolar bone protection in image-guided high-dose-rate interstitial brachytherapy for tongue cancer.

Material and methods: We treated 6 patients and delivered 5,400 cGy in 9 fractions using a lead block. Effects of lead block (median thickness, 4 mm) on dose attenuation by distance were visually examined using TG-43 formalism-based dose distribution curves to determine whether or not the area with the highest dose is located in the alveolar bone, where there is a high-risk of infection. Dose re-calculations were performed using TG-186 formalism with advanced collapsed cone engine (ACE) for inhomogeneity correction set to cortical bone density for the whole mandible and alveolar bone, water density for clinical target volume (CTV), air density for outside body and lead density, and silastic density for lead block and its' silicon replica, respectively.

Results: The highest dose was detected outside the alveolar bone in five of the six cases. For dose-volume histogram analysis, median minimum doses delivered per fraction to the 0.1 cm^3 of alveolar bone (D0.1cm$^3_{TG-43, ACE-silicon, and ACE-lead}$) were 344.3 (range, 262.9-427.4) cGy, 336.6 (253.3-425.0) cGy, and 169.7 (114.9-233.3) cGy, respectively. D0.1cm$^3_{ACE-lead}$ was significantly lower than other parameters. No significant difference was observed between CTV-related parameters.

Conclusions: The results suggested that using a lead block for alveolar bone protection with a thickness of about 4 mm, can shift the highest dose area to non-alveolar regions. In addition, it reduced D0.1cm^3 of alveolar bone to about half, without affecting tumor dose.
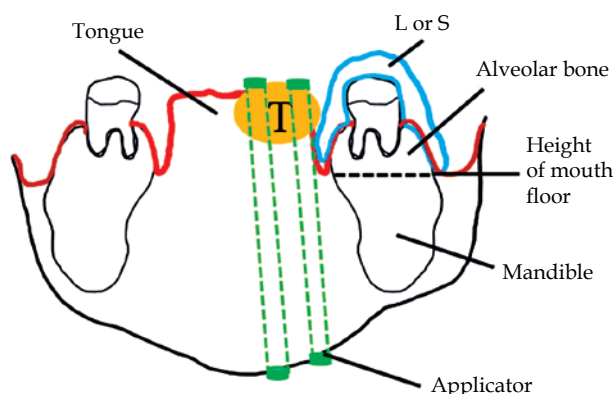
Key words: brachytherapy, tongue cancer, lead block, bone protection, inhomogeneity correction.

Address for correspondence: Hironori Akiyama, Department of Oral Radiology, Osaka Dental University, 1-5-17 Otemae, Chuo-ku, Osaka, Osaka, 540-0008, Japan, phone: +81-90-5894-3937, fax: +81-6-6910-1075, ✉ e-mail: ddiisbt@gmail.com

Purpose

High-dose-rate interstitial brachytherapy (HDR ISBT) provides good results in the treatment of tongue cancer [1]. Important adverse reactions to this therapy include mandibular osteonecrosis [2], which requires mandibular dose reduction to prevent its' occurrence. To achieve this, a lead block is used during treatment sessions to cover the alveolar region of the mandible, which is a part of the mandible where the teeth are implanted and protected by a lead block or silicon replica, so called 'alveolar bone', close to the tongue (Figure 1) [3]. Our lead block was coated with rubber to prevent unexpected radiation exposure due to scattering radiation [4] and toxicity of lead. The lead block reduces dose received by alveolar bone through two mechanisms. One is the spacing effect of inverse square law of distance provided by thickness of the lead block that separates the alveolar bone from the tongue. The other is the blocking effect from γ-ray absorption provided by density of the lead block, which has a large atomic number. Inoue et al. documented benefits of the spacing effect [1]; however, no studies have been performed on how much the dose is attenuated. Recently, Murakami *et al*. showed a dose-rate reduction assessment for a modular spacer, although which part of the mandible actually received the highest dose has not been investigated [5]. In addition, our dose calculations have been made for a long time using a formalism provided by the American Association of Physicists in Medicine Task Group No. 43 (TG-43) [6-8]. This dose calculation assumes an infinite space filled with water, and therefore does not consider the anatomy or density of tumor or organs at risk. For this reason, the influence of blocking effect provided by the lead block is no not taken into account by TG-43 formalism. Recent advances in diagnostic imaging technology have enabled us to administer doses under imaging guidance to anatomical structures in image-guided (IG) HDR ISBT [4]. This allows the doses delivered to the tumor and mandible to be determined using dose-volume histogram (DVH) [9]. However, dose calculation still relies on TG-43 formalism, meaning that no inhomogeneity correction is applied; therefore, mandibular/tumor dose calculations may not be accurate.

The above-mentioned problems can be overcome by using calculation methods provided by TG-186, which does correct for inhomogeneity. This is made possible using model-based dose calculation algorithms, which were also introduced into brachytherapy (BT) [10]. Such algorithms include grid-based Boltzmann equation solvers, Monte Carlo simulations, and collapsed cone convolution. To date, reports have been published that compared dose calculation results obtained using model-based dose calculation algorithms, such as grid-based Boltzmann equation solvers and Monte Carlo simulations, with those obtained using TG-43 formalism for BT in the head and neck region [5, 11, 12]. However, to the best of our knowledge, there have been no reports on the use of collapsed cone convolution for dose calculation in the head and neck BT. Dose calculation using collapsed cone convolution has been used for many years in external irradiation [13]. Advanced collapsed cone engine (ACE) is a collapsed cone convolution algorithm integrated into OncentraBrachy treatment planning system version 4.5.3 (Elekta, Veenendaal, The Netherlands) for use in BT [14]. Ma *et al*. reported that ACE demonstrated good agreement with Monte Carlo simulations in most clinically relevant regions (e.g., prostate, breast, and chest wall) [14], suggesting the validity of dose calculation using ACE. Inhomogeneity correction using ACE has been documented in gynecology field [15], but not in the field of head and neck cancer as yet.

The purpose of this study was to evaluate the effectiveness of a lead block for alveolar bone protection through not only the spacing but also blocking effects as well as the effect on tumor dose in IG-HDR ISBT for tongue cancer. We retrospectively analyzed DVH parameters of previously treated tongue cancer patients created using a TG-43-based calculation, because there was no model-based dose calculation algorithms at that time.

Material and methods

This multicenter study was conducted with an approval from the Research Ethics Committee of Osaka Medical and Pharmaceutical University, approval No.: CL-514 (2232).

Patients

The present study involved six patients who underwent IG-HDR ISBT for tongue cancer at the National Hospital Organization Osaka National Hospital, between September, 2010 and August, 2012. Male : female ratio was 4 : 2, median age was 60 years (range, 39-84 years), T2 : T3 ratio was 5 : 1, and histological type was squamous cell carcinoma in all cases.

Image-guided high-dose-rate interstitial brachytherapy

After 6-15 catheters were inserted under general anesthesia, computed tomography (CT) scanning was performed for treatment planning. Because the lead

Fig. 1. Schema of coronal imaging of the oral cavity. Alveolar bone is part of the mandible, where the teeth are implanted and protected by a lead block or silicon replica
T – tumor; L – lead block; S – silicon replica

block used for treatment sessions would produce imaging artifacts, a replica made from dental silicon impression material Coltflax (Coltene/Whaledent AG, Altstätten, Switzerland) was used during CT scanning. Images were transferred to OncentraBrachy treatment planning system, version 4.1, to delineate clinical target volume (CTV) and whole mandible for dose calculation using TG-43 formalism. The size of calculation grid was 1 mm at minimum. With DVH, the treatment plan was adjusted such that the minimum dose delivered to 90% of CTV ($D90_{TG-43}$) would be equal to or greater than the planning-aim dose, the percentage of CTV that received 100% of planning-aim dose ($V100_{TG-43}$) would be equal to or greater than 90%. The minimum dose delivered to 0.1 cm^3 of the whole mandible ($D0.1cm^3_{TG-43}$) was used to evaluate mandibular dose. There has been no research that reported an association between $D0.1cm^3$ and mandibular osteonecrosis in HDR-BT at present. Fujita *et al.* reported on patients treated with a combination of external irradiation of 30 Gy and low-dose-rate (LDR) BT of 60 Gy, which was a threshold of mandibular bone complication [16]. Combination of external irradiation of 30 Gy and LDR-BT of 60 Gy to normal tissue was almost 102 Gy in equivalent dose in 2 Gy fraction (repair half-time = 2 hours, α/β = 3), and that of our planning-aim dose of 54 Gy was 105 Gy (repair half-time = 2 hours, interfraction intervals = 6 hours, α/β = 3) [17, 18]. Based on this data, our policy of dose constraints for mandible was that $D0.1cm^3_{TG-43}$ was less than planning-aim dose of 600 cGy per fraction (total dose, 5,400 cGy). We implanted catheters to the patients on the first day in the morning, and then we irradiated them only once in the afternoon. We irradiated twice a day from the next day, for a total dose of 5,400 cGy. During treatment session, the rubber coted lead block was used to cover alveolar bone close to the lesion that received the highest dose across the whole mandible, which was at high-risk of infection.

Spacing effect of the lead block

Dose distribution curves created using TG-43-based calculations were used to visually determine whether or not the area with the highest dose was located in the alveolar bone. Treatment planning system was also used to measure thickness of the block at shortest distance between the applicator and alveolar bone.

Re-calculation using collapsed cone engine

To consider density of the lead block and other anatomical structures, dose re-calculation was performed using ACE. CT images used for treatment planning were transferred to ACE, and the block and facial contour were additionally registered on the images. Alveolar bone that was covered by the block was also registered to investigate more direct impact of the lead block. For inhomogeneity correction with ACE, a cortical bone density of 1.92 g/cm^3 was assigned to the whole mandible and alveolar bone. Generally, bones are divided into outer high-density cortical bone and inner low-density spongiosa. Spongiosa is composed of 33% cortical bone and 67% marrow [19]. In order to calculate heterogeneity cor-

rection by ACE, it was necessary to assign density based on the product label of ACE after contouring each substance, rather than being calculated based on CT values. However, it would be difficult to distinguish and contour cortical bone, spongiosa, and marrow on CT. Moreover, there was no data of density of spongiosa on the product label of ACE. Additionally, we evaluated mandibular dose by $D0.1cm^3$, and the dose might be located in outer high-density cortical bone close to radiation source. For these reasons, we thought it was all right that a cortical bone density was assigned to the whole mandible and alveolar bone. A water density of 1.0 g/cm^3 was assigned to CTV, and an air density of 0.00121 g/cm^3 was allocated to outside the body. In the maxillofacial region, there are two air-containing regions, such as oral cavity and maxillary sinus. As for the oral cavity, gauze soaked 2% lidocaine (Xylocaine® jelly 2%) was inserted for the purpose of mouth opening to avoid exposure of the maxilla. The reason for infiltrating the gauze with 2% lidocaine was to give the gauze almost the same shielding ability as water, and to relieve the pain of putting the gauze in the mouth. Furthermore, saliva was also infiltrated into the gauze. From these considerations, we thought that oral cavity, especially around CTV, could be regarded as water in dose calculation. Regarding the maxillary sinuses, most of them were not visualized on the image, because CT were taken only up to the vicinity of the hard palate, as the maxillary sinuses were far from CTV due to the mouth opening and considering the patient's exposure. Therefore, it was not possible to calculate dose considering the effects of air in the maxillary sinuses. For the lead block and its' silicon replica, density of lead (11.1 g/cm^3) and density of silastic (1.12 g/cm^3) were assigned, respectively. These density values were based on the product label of ACE. Using DVH, the following parameters were calculated: the minimum dose delivered to the 0.1 cm^3 ($D0.1cm^3_{ACE-silicon \text{ or } ACE-lead}$) of the alveolar bone and whole mandible; the minimum dose delivered to 90% of CTV ($D90_{ACE-silicon \text{ or } ACE-lead}$); and the percentage of CTV that received 100% of the planning-aim dose ($V100_{ACE-silicon \text{ or } ACE-lead}$). The size of calculation grid was 1 mm at minimum.

Statistical analysis

Normality of data was examined using Kolmogorov-Smirnov test. Calculation results using TG-43, ACE-silicon, and ACE-lead were compared for each DVH parameter. Repeated measures one-way analysis of variance and Tukey's post-hoc multiple comparison test were applied for parametric comparisons. Friedman's test and Dunn's *post-hoc* multiple comparison test were used for non-parametric comparisons. Correlation between thickness of the block and dose ratio in $D0.1cm^3$ ($D0.1cm^3_{ACE-silicon \text{ or } ACE-lead}/D0.1cm^3_{TG-43}$) of the whole mandible and alveolar bone was examined using Spearman's correlation coefficient.

Differences were considered statistically significant at $p < 0.05$. All analyses were performed using GraphPad Prism version 5.01 for Windows (GraphPad Software, San Diego, CA, USA).

Table 1. Area with the highest dose across the whole mandible as determined visually on dose distribution curves based on the American Association of Physicists in Medicine Task Group 43 formalism
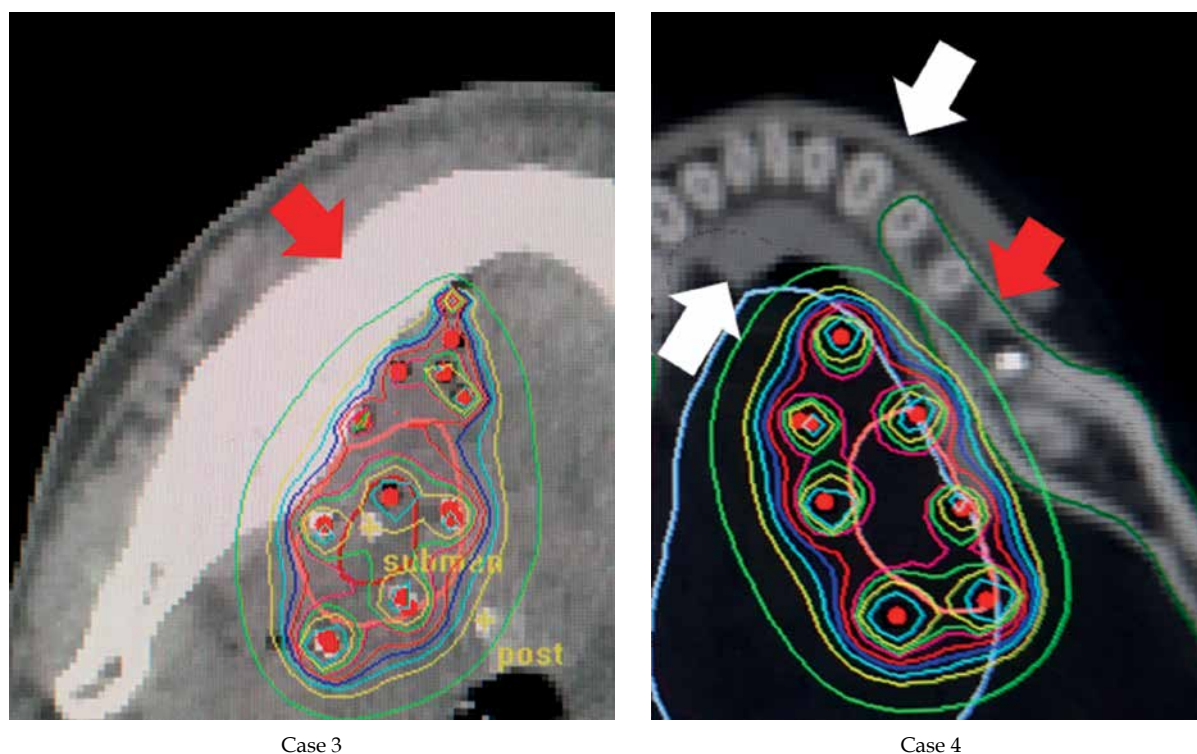
| Case	Area
1	Ramus of mandible
2	Below alveolar bone
3	Below alveolar bone
4	Alveolar bone
5	Below alveolar bone
6	Ramus of mandible

Results

The areas with the highest dose across the whole mandible, as determined visually on TG-43-based dose distribution curves, are shown in Table 1, and representative dose distribution curves are shown in Figure 2. The highest dose was detected in non-alveolar bone in five of the six cases. In case 3, 90% of the planning-aim dose was delivered to below the alveolar bone (Figure 2). Case 4 was the only case, in which the highest dose was detected in the alveolar bone, with 80% of the planning-aim dose

reaching the cortical bone in the alveolar bone. The median $D0.1cm^3_{TG-43 \text{ or } ACE\text{-silicon or } ACE\text{-lead}}$ values of the alveolar bone were 344.3 (range, 262.9-427.4) cGy, 336.6 (range, 253.3-425.0) cGy, and 169.7 (range, 114.9-233.3) cGy, respectively, with $D0.1cm^3_{ACE\text{-lead}}$ being significantly lower than the other two parameters in the alveolar bone (Figure 3A). The dose ratio in median $D0.1cm^3$ ($D0.1cm^3_{ACE\text{-silicon or } ACE\text{-lead}}/D0.1cm^3_{TG-43}$) of the alveolar bone were 97.8% and 49.3%, respectively, indicating that the dose in the lead density setting was attenuated to approximately half of that calculated using TG-43 formalism. Figure 4 shows ACE-based dose distribution curves of the case, in which the highest dose across the whole mandible was detected in the alveolar bone (case 4 from Figure 2), as determined visually on TG-43-based dose distribution curves. When the block was set to have silicon density (ACE-silicon), 80% of the planning-aim dose reached the cortical bone in the alveolar bone surface, as in the case of TG-43-based calculation (case 4 from Figure 2). In contrast, when the block was set to the density of lead (ACE-lead), the dose delivered to the cortical bone in the alveolar bone surface was attenuated to 50% of the planning-aim dose.

For the whole mandible, the median $D0.1cm^3_{TG-43 \text{ or } ACE\text{-silicon or } ACE\text{-lead}}$ values were 485.2 (range, 391.2-528.5) cGy, 504.6 (range, 362.9.6-570.0) cGy, and 444.6 (range, 209.5-546.1) cGy, respectively, with no significant difference between calculation methods (Figure 3B).

Case 3   Case 4

Fig. 2. Representative dose distribution curves for a case, where the highest dose across the whole mandible was detected in non-alveolar bone (case 3), and for a case, where the highest dose area was in the alveolar bone (case 4). Calculations were made using a formalism provided by the American Association of Physicists in Medicine Task Group 43. Red arrows indicate the whole mandible, white arrows indicate the block, a blue curve indicates 90% of the planning-aim dose, and a light blue curve indicates 80% of the planning-aim dose. In case 3, 90% of the planning-aim dose (blue curve) was delivered to the cortical bone below the alveolar bone due to the spacing effect of the block. In case 4, due to an insufficient spacing effect, 80% of the planning-aim dose (light blue curve) was delivered to the cortical bone in the alveolar bone surface

ACE-silicon
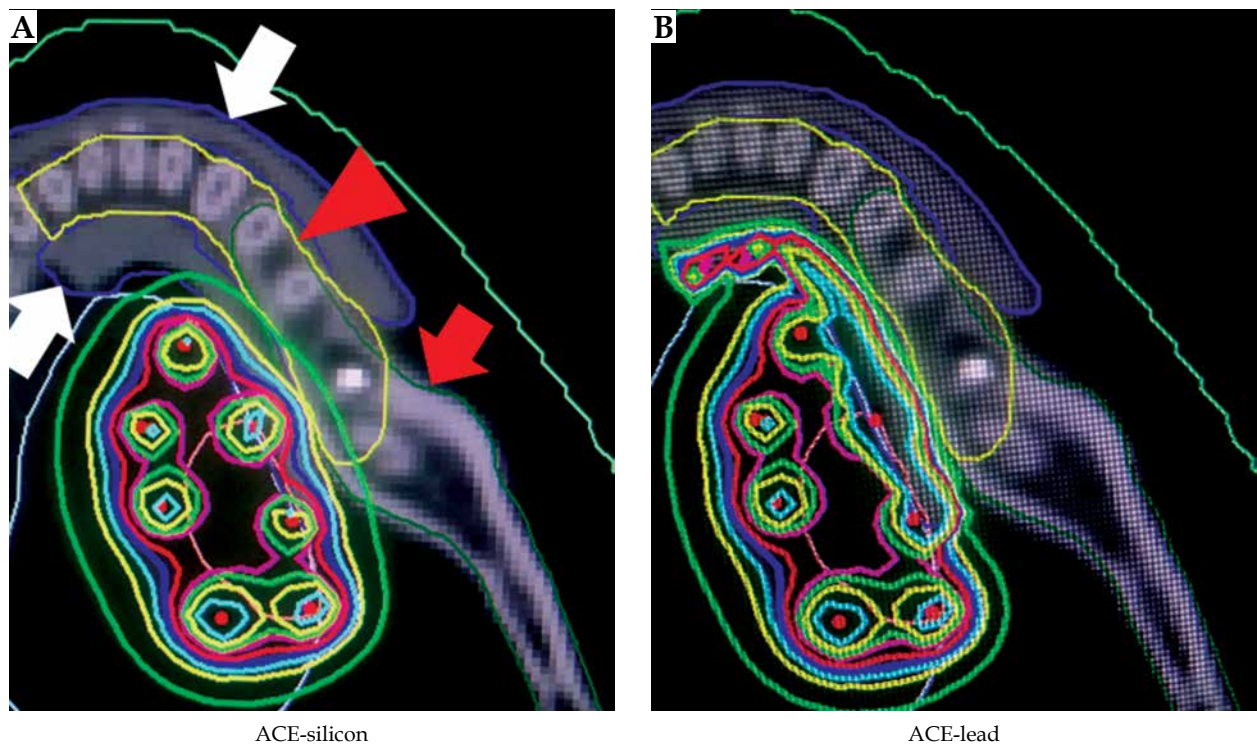
ACE-lead

Fig. 3. Minimum dose delivered to 0.1 cm^3 of the alveolar bone (**A**) and the whole mandible (**B**) (D0.1cm^3_X). X = TG-43, ACE-silicon, or ACE-lead, which were calculated using the Association of Physicists in Medicine Task Group 43 formalism, advanced collapsed cone engine (ACE) with a silicon density setting, and ACE with a lead density setting, respectively. Asterisk indicates a significant difference ($p < 0.05$)

The median thickness of the block was 4.2 (range, 2.9-4.4) mm, and its' relationship with the dose ratio in D0.1cm^3 (D0.1cm$^3_{ACE-silicon \ or \ ACE-lead}$/D0.1cm$^3_{TG-43}$) in the whole mandible and the alveolar bone is shown in Figure 5. There was a significant negative correlation between the thickness of the block and the D0.1cm$^3_{ACE-lead}$/

D0.1cm$^3_{TG-43}$ of the alveolar bone (Spearman's correlation coefficient = −0.88, $p = 0.03$).

For the CTV, the median D90$_{TG-43 \ or \ ACE-silicon \ or \ ACE-lead}$ values were 652.0 (range, 600.9-687.0) cGy, 653.4 (range, 625.9.6-720.5) cGy, and 651.5 (range, 625.0-715.1) cGy, respectively, and those of V100$_{TG-43 \ or \ ACE-silicon \ or \ ACE-lead}$
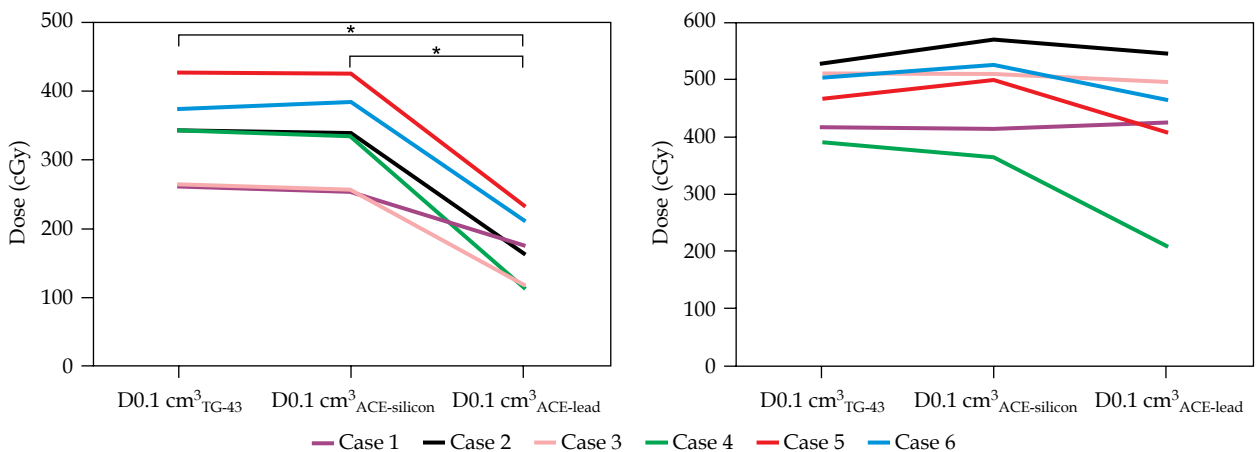
Fig. 4. Dose distribution curves based on re-calculations using the advanced collapsed cone engine (ACE) for a case, where the highest dose was detected in the alveolar bone (case 4 from Figure 1). A red arrow indicates the whole mandible, a red arrowhead indicates the alveolar bone, white arrows indicate the block, a light blue curve indicates 80% of the planning-aim dose, and a green curve indicates 50% of the planning-aim dose. When the silicon density was assigned to the block (ACE-silicon), the light blue curve indicating 80% of the planning-aim dose was in contact with the cortical bone in the alveolar bone surface, similar to the results obtained using the American Association of Physicists in Medicine Task Group 43 formalism (case 4 from Figure 1). In contrast, when the lead density was assigned to the block (ACE-lead), the green curve indicating 50% of the planning-aim dose was in contact with the cortical bone in the alveolar bone surface
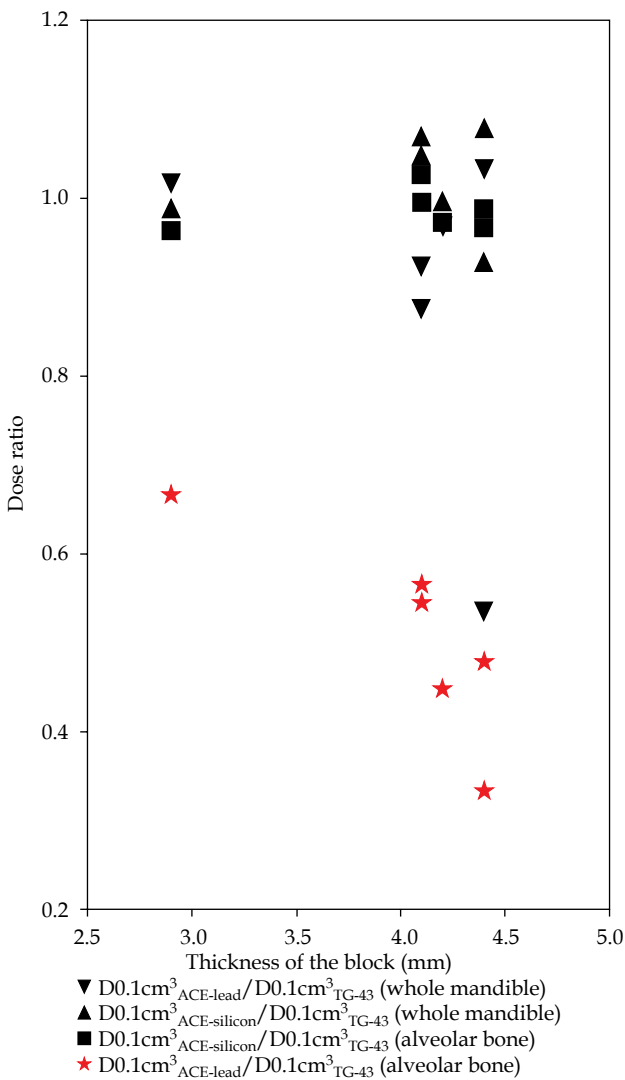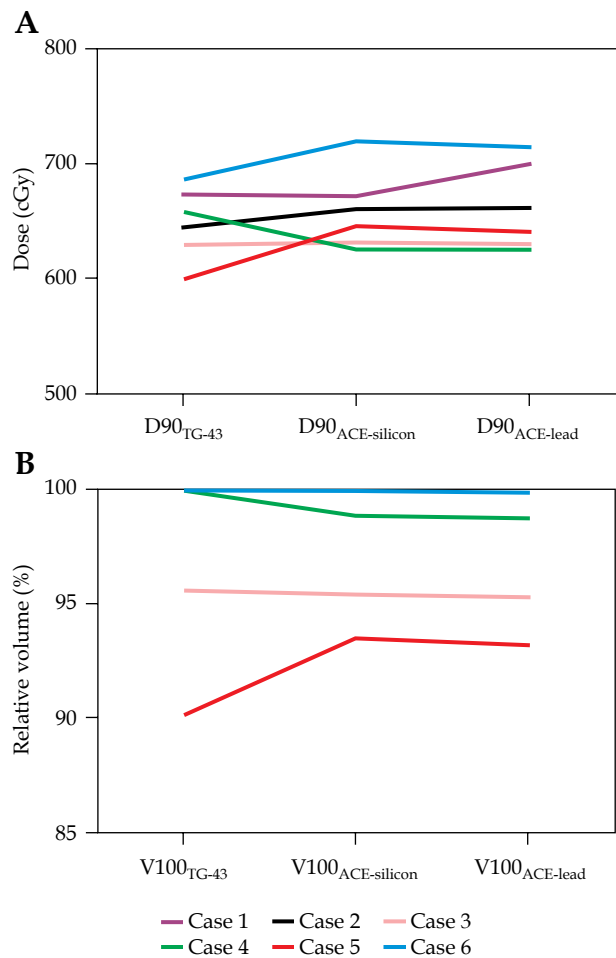
Fig. 5. Correlation between thickness of the block and dose ratio. $D0.1cm^3_X$: The minimum dose delivered to 0.1 cm^3 of the whole mandible or the alveolar bone. X = TG-43, ACE-silicon, or ACE-lead were calculated using the Association of Physicists in Medicine Task Group 43 formalism, advanced collapsed cone Engine (ACE) with the silicon density setting, and ACE with the lead density setting, respectively. A red star indicates a significant negative correlation, with Spearman's correlation coefficient of 0.88, $p < 0.05$

Fig. 6. Minimum dose delivered to 90% of the clinical target volume ($D90_X$, **A**) and the percentage of the clinical target volume that received 100% of the planning-aim dose ($V100_X$, **B**). X = TG-43, ACE-silicon, or ACE-lead were calculated using the Association of Physicists in Medicine Task Group 43 formalism, advanced collapsed cone engine (ACE) with the silicon density setting, and ACE with the lead density setting, respectively. No significant differences in dose values were observed between calculation methods

were 100.0% (range, 90.1-100.0%) 99.5% (range, 93.5-100.0%), and 99.3% (range, 93.2-100.0%), with no significant differences for either D_{90} or V_{100} (Figure 6).

Discussion

Murakami *et al*. examined distance-dependent attenuation of γ-rays from an HDR radiation source, and reported that for a shortest distance between the mandible and the reference point (e.g., 10 mm from the source or 5 mm from 60 Gy reference point), the dose reduction can reach 51.2% (30.7 Gy of 60 Gy dose at reference point) [5]. However, there have been no reports describing which specific

area receives the highest dose in this setting. In HDR-BT for tongue cancer, alveolar bone is likely to receive the highest dose across the whole mandible due to its' close proximity to the lesion. Evidence has also suggested an association between mandibular osteonecrosis after radiation therapy and oral hygiene status [20]. Treating of existing oral disease, and stabilizing oral health before and after cancer therapy, may decrease the risk of osteoradionecrosis. The goal is to minimize the need of invasive interventions (e.g., extraction) as well as dental inflammatory disease/infection during and after radiation therapy for the life of patient [21]. Therefore, if the spacing effect of the lead block was to shift the highest dose area to an area other than alveolar bone, where teeth as the source of infection are present, it should reduce the occurrence of mandibular osteonecrosis. This led to our decision to cover the alveolar bone with a lead block during treat-

ment sessions, because this is the area where the dose was highest across the mandible with a high-risk of infection. In the visual evaluation of TG-43-based dose distribution curves, the highest dose was detected outside the alveolar bone in five out of six cases, suggesting a benefit of the spacing effect provided by the lead block covered using our method.

We have reported previously on mandibular dose calculation in HDR-BT for tongue cancer [4, 9]. However, in these reports, dose calculations were based on TG-43 method, therefore, the exact dose values were unknown. Peppa *et al.* used Monte Carlo simulations to calculate mandibular doses in the head and neck cancer, but they did not consider the effect of a lead block for alveolar bone protection [12]. The present study was designed to overcome the limitations of previous studies. In terms of materials used for the block, dental silicone impression materials are advantageous in that they produce fewer artifacts during CT scanning, are easy to mold the shape of the mandible, and are not harmful to human body. Therefore, in the present study, an analysis was also performed using dental silicon impression material. This was possible because during CT scanning for treatment planning, we used a replica made of dental silicon impression material, which had the same shape as the lead block used during treatment sessions.

In the DVH analysis of the alveolar bone, $D0.1cm^3$ calculated using ACE with the block set to lead density was significantly reduced (by 49%) compared with those calculated using TG-43 formalism, or with the block set to silicon density. These results suggested that radiation dose to the alveolar bone can be reduced by the blocking effect, even when the spacing effect is insufficient. In fact, in case 4, where the spacing effect was insufficient, visual evaluation of the ACE-based dose distribution curves revealed that 80% of the planning-aim dose contacted the cortical bone in the alveolar bone surface in the silicon density setting, as when it was calculated using TG-43 formalism, whereas in the lead density setting, the dose was reduced to 50% of the planning-aim dose, in agreement with the DVH analysis results (Figure 4). In practice, the dose to tissues in contact with lead might be higher because of scattered radiation from the lead. Lliso *et al.* reported that higher doses might be expected when an internal lead shielding is used in case of HDR ^{192}Ir treatment, where apart from reduction, a strong dose enhancement is observed in the tissue on the backscatter side adjacent to the lead slab, and also in the forward scatter side [22]. Therefore, a few millimeters of bolus to the lead to avoid the overdose of the tissue in contact with the lead is necessary. Lliso *et al.* also reported that minimum bolus thickness that must be added in order to remove the dose contamination resulted in values of 0.5 mm and 1 mm in the backward and forward radiation direction, respectively. GEC-ESTRO recommendations for BT of squamous cell carcinoma of the head and neck reported that the shielding system consisted of a 2 mm thick lead shield wrapped in plastic protection [23]. In reality, our lead block was coated with rubber to prevent unexpected radiation exposure due to scattering

radiation. However, in this study, a part of rubber density around lead density was not considered. This was because in the treatment planning, CT silicon replica was used in consideration of artifacts, so it was impossible to separate the part of rubber density from the lead density part on the image. Even if it could be done, it would be difficult to contour the rubber part separately because the width of rubber was too narrow. In addition, there is no data of density of rubber on the product label of ACE. Therefore, in this study, we would like to assign the lead density to all blocks. As a result, there was a high-dose area around the lead, which can be seen in Figure 4, when the lead density was assigned to the block (ACE-lead). However, due to the blocking effect of the lead, the dose of bone surface was reduced from 80% planning-aim dose in silicon density setting to 50% planning-aim dose in lead density setting. Although the actual dose was expected to decrease further, we believed that the blocking effect of lead was almost confirmed even in our setting. For these reasons, in this study, we thought it was good enough to assign the lead density to all blocks. As for the blocking effect in HDR radiation source, Murakami *et al.* demonstrated using Monte Carlo simulations that when 4 mm thick lead was placed 10 mm away from reference point, the dose was reduced to 30.5% (single-plane implant) and 30.2% (double-plane implant) of the dose without the lead [5]. Actual measurement of blocking effect of the lead has been reported by Kudoh *et al.* [24]. They used 5 cm × 5 cm lead and acrylic plates, and evaluated their blocking effect quantitatively using a thermoluminescence dosimeter. Their results showed that the dose with a 4 mm lead and 3 mm acrylic plate was 27.7% of that with a 7 mm acrylic plate. The median thickness of the lead block used in the present study was 4.2 mm, which is almost the same as that used in the above-mentioned previous study [5, 24]. The DVH analysis showed that the median $D0.1cm^3$ of the alveolar bone calculated using ACE with the lead density setting was about 49% of that calculated using TG-43 formalism. Thus, the blocking effect demonstrated in the present study was smaller than that in the previous study. This may be because the previous study did not consider density or anatomy of the human body components, and thus did not consider the effects of scattered radiation from the mandible and other structures, resulting in lower dose calculations compared with ours.

Regarding the whole mandibular dose, in our previous study involving five patients who underwent HDR-BT for tongue cancer, we obtained a mean $D0.1cm^3$ of 480.6 cGy as calculated using TG-43 formalism [4], which was roughly equivalent to a median $D0.1cm^3$ of 485.2 cGy in the present study. In the whole mandible, no significant difference was observed in $D0.1cm^3$ calculated between using TG-43 formalism and ACE assigned to the lead and silicon density settings. As shown in Figure 3B, one case (case 4) had a $D0.1cm^3_{ACE-lead}$ that was substantially lower than the other parameters, and in this case, the area with the highest dose was in the alveolar bone covered by the lead block, as shown in Table 1. This suggested the benefit of the blocking effect of the lead block

when the alveolar bone is exposed to the highest dose, even in dose calculation for the whole mandible.

There was a significant negative correlation between the thickness of the block and the $D0.1cm^3_{ACE-lead}$/ $D0.1cm^3_{TG-43}$ of the alveolar bone. In the alveolar bone, increasing the thickness of the lead block will increase the blocking effect. However, the thicker the lead block, the more discomfort the patient would feel. Future studies should examine the range of lead thickness tolerable for patients and monitor the incidence of mandibular osteonecrosis over a longer follow-up period.

There have been several reports on inhomogeneity correction in head and neck BT, and these reports suggested a limited effect in CTV of inhomogeneity correction. Siebert et al. reported that dosimetric indices of D_{90} and V_{100} for CTV were about 3% lower for grid-based Boltzmann solver compared with TG-43-based computation. Patients showed small variations and, with clinical use of these indices, prescription doses remained unchanged for HDR in head and neck BT for the time being [11]. Using Monte Carlo simulation, Peppa et al. reported significant differences in planning target volume in an analysis of relative DVH indices, due to consistent dose overestimation using TG-43 formalism, although these differences were not of sufficient magnitude or range to warrant any change in treatment planning practice [12]. However, these studies did not use any alveolar bone protection. When such a block is used, CTV may be exposed to scattered radiation from the block due to proximity of the block to the tongue. In the present study, however, there was no significant difference in the V_{100} or D_{90} parameters, regardless of the density setting of the block.

Limitations of this study include that no actual dose measurement was performed. Future studies should compare calculated and measured results obtained in the same environment using, for example, an oral equivalent phantom. Additionally, the number of the patients in this study was too small, and it was difficult to draw firm conclusions. Further studies with a larger number of patients are therefore required.

Conclusions

Our results suggested that the use of a lead block with a thickness of about 4 mm for alveolar bone protection can shift the highest dose area to non-alveolar bone through the spacing effect. In addition, it reduced the $D0.1cm^3$ of the alveolar bone to about half without affecting the tumor dose through the blocking effect.

Ethics

This multicenter study was conducted with an approval from the Research Ethics Committee of Osaka Medical and Pharmaceutical University (Approval No. CL-514(2232)).

Disclosure

Ken Yoshida has received an honorarium from Chiyoda Technol Corporation. The other authors report no conflict of interest.

References

1. Inoue T, Inoue T, Yoshida K et al. Phase III trial of high- vs. low-dose-rate interstitial radiotherapy for early mobile tongue cancer. *Int J Radiat Oncol Biol Phys* 2001; 51: 171-175.
2. Shimizutani K, Inoue T, Inoue T et al. Late complications after high-dose-rate interstitial brachytherapy for tongue cancer. *Oral Radiol* 2005; 21: 1-5.
3. Akiyama H, Yoshida K, Yamazaki H et al. High-dose-rate interstitial brachytherapy for mobile tongue cancer: preliminary results of a dose reduction trial. *J Contemp Brachytherapy* 2014; 6: 10-14.
4. Yoshida K, Takenaka T, Akiyama H et al. Three-dimensional image-based high-dose-rate interstitial brachytherapy for mobile tongue cancer. *J Radiat Res* 2014; 55: 154-161.
5. Murakami S, Verdonschot RG, Kakimoto N et al. Preventing complications from high-dose rate brachytherapy when treating mobile tongue cancer via the application of a modular lead-lined spacer. *PLoS One* 2016; 11: e0154226.
6. Akiyama H, Yoshida K, Shimizutani K et al. Dose reduction trial from 60 Gy in 10 fractions to 54 Gy in 9 fractions schedule in high-dose-rate interstitial brachytherapy for early oral tongue cancer. *J Radiat Res* 2012; 53: 722-726.
7. Nath R, Anderson LL, Luxton G et al. Dosimetry of interstitial brachytherapy sources: recommendations of the AAPM Radiation Therapy Committee Task Group No. 43. American Association of Physicists in Medicine. *Med Phys* 1995; 22: 209-234.
8. Rivard MJ, Coursey BM, DeWerd LA et al. Update of AAPM Task Group No. 43 Report: A revised AAPM protocol for brachytherapy dose calculations. *Med Phys* 2004; 31: 633-674.
9. Akiyama H, Major T, Polgar C et al. Dose-volume analysis of target volume and critical structures in computed tomography image-based multicatheter high-dose-rate interstitial brachytherapy for head and neck cancer. *J Contemp Brachytherapy* 2017; 9: 553-560.
10. Beaulieu L, Carlsson Tedgren A, Carrier JF et al. Report of the Task Group 186 on model-based dose calculation methods in brachytherapy beyond the TG-43 formalism: current status and recommendations for clinical implementation. *Med Phys* 2012; 39: 6208-6236.
11. Siebert FA, Wolf S, Kovacs G. Head and neck (192)Ir HDR-brachytherapy dosimetry using a grid-based Boltzmann solver. *J Contemp Brachytherapy* 2013; 5: 232-235.
12. Peppa V, Pappas E, Major T et al. On the impact of improved dosimetric accuracy on head and neck high dose rate brachytherapy. *Radiother Oncol* 2016; 120: 92-97.

13. Ahnesjo A. Collapsed cone convolution of radiant energy for photon dose calculation in heterogeneous media. *Med Phys* 1989; 16: 577-592.

14. Ma Y, Lacroix F, Lavallee MC et al. Validation of the Oncentra Brachy Advanced Collapsed cone Engine for a commercial (192)Ir source using heterogeneous geometries. *Brachytherapy* 2015; 14: 939-952.

15. Abe K, Kadoya N, Sato S et al. Impact of a commercially available model-based dose calculation algorithm on treatment planning of high-dose-rate brachytherapy in patients with cervical cancer. *J Radiat Res* 2018; 59: 198-206.

16. Fujita M, Hirokawa Y, Kashiwado K et al. An analysis of mandibular bone complications in radiotherapy for T1 and T2 carcinoma of the oral tongue. *Int J Radiat Oncol Biol Phys* 1996; 34: 333-339.

17. Pop LA, van den Broek JF, Visser AG et al. Constraints in the use of repair half times and mathematical modelling for the clinical application of HDR and PDR treatment schedules as an alternative for LDR brachytherapy. *Radiother Oncol* 1996; 38: 153-162.

18. Joiner M, Kogel AVD (Eds.). Basic Clinical Radiobiology 4th edition. CRC Press, Boca Raton 2009: 109-113.

19. White DR, Booz J, Griffith RV et al. ICRU Report 44: Tissue Substitutes in Radiation Dosimetry and Measurement. *J ICRU* 1989; 23.

20. Katsura K, Sasai K, Sato K et al. Relationship between oral health status and development of osteoradionecrosis of the mandible: a retrospective longitudinal study. *Oral Surg Oral Med Oral Pathol Oral Radiol Endod* 2008; 105: 731-738.

21. Sroussi HY, Epstein JB, Bensadoun RJ et al. Common oral complications of head and neck cancer radiation therapy: mucositis, infections, saliva change, fibrosis, sensory dysfunctions, dental caries, periodontal disease, and osteoradionecrosis. *Cancer Med* 2017; 6: 2918-2931.

22. Lliso F, Granero D, Perez-Calatayud J et al. Dosimetric evaluation of internal shielding in a high dose rate skin applicator. *J Contemp Brachytherapy* 2011; 3: 32-35.

23. Mazeron JJ, Ardiet JM, Haie-Méder C et al. GEC-ESTRO recommendations for brachytherapy for head and neck squamous cell carcinomas. *Radiother Oncol* 2009; 91: 150-156.

24. Kudoh T, Ikushima H, Honda E. Shielding effect of a customized intraoral mold including lead material in high-dose-rate 192-Ir brachytherapy for oral cavity cancer. *J Radiat Res* 2012; 53: 130-137.